Laser locking to the ^{199}Hg $^1S_0 - {}^3P_0$ clock transition with $5.4 \times 10^{-15}/\sqrt{\tau}$ fractional frequency instability

J. J. McFerran,[1,*] D. V. Magalhães,[2] C. Mandache,[1] J. Millo,[1] W. Zhang,[1] Y. Le Coq,[1] G. Santarelli,[1] and S. Bize[1,3]

[1]LNE-SYRTE, Observatoire de Paris, CNRS, UPMC, 61 Avenue de l'Observatoire, 75014 Paris, France

[2]Escola de Engenharia de São Carlos, Universidade de São Paulo, São Carlos 13566-590, Brazil

e-mail: sebastien.bize@obspm.fr

*Corresponding author: john.mcferran@obspm.fr

Received May 17, 2012; accepted July 5, 2012;
posted July 13, 2012 (Doc. ID 166404); published August 16, 2012

With ^{199}Hg atoms confined in an optical lattice trap in the Lamb–Dicke regime, we obtain a spectral line at 265.6 nm for which the FWHM is ~15 Hz. Here we lock an ultrastable laser to this ultranarrow $^1S_0 - {}^3P_0$ clock transition and achieve a fractional frequency instability of $5.4 \times 10^{-15}/\sqrt{\tau}$ for $\tau \le 400$ s. The highly stable laser light used for the atom probing is derived from a 1062.6 nm fiber laser locked to an ultrastable optical cavity that exhibits a mean drift rate of -6.0×10^{-17} s^{-1} (-16.9 mHz s^{-1} at 282 THz) over a six month period. A comparison between two such lasers locked to independent optical cavities shows a flicker noise limited fractional frequency instability of 4×10^{-16} per cavity.

OCIS codes: 300.6360, 300.6540, 120.3940.

Optical atomic frequency references are making significant advances in terms of accuracy [1–5] and stability [6–8] across a range of atomic species, which is important for continued investigation into a potential redefinition of the Système-Internationale (SI) second, and into possible variations of fundamental constants [9]. It also motivates research in establishing low-noise frequency links between various atomic clocks over distant Earth locations via optical fibers [10,11] and space [12,13]. In previous work we established the potential of the $(6s^2)\ {}^1S_0 - (6s6p)\ {}^3P_0$ clock transition in ^{199}Hg as a high-accuracy atomic frequency reference [14]. All the associated frequency measurements to date have relied on line-center determinations from spectral profile measurements. Here we lock a probe laser to the ^{199}Hg clock transition for the first time and deduce the fractional frequency stability, $\sigma_y(\tau)$, demonstrating a $\tau^{-1/2}$ dependence typical of atomic clocks. With $\sigma_y(\tau)$ integrating down to few times 10^{-16} within several hundred seconds, accuracies in the 10^{-17} range are foreseeable in forthcoming work. We also present $\sigma_y(\tau)$ measurements between two fused-silica mirror based high-finesse optical cavities, one of which is used for ^{199}Hg spectroscopy, demonstrating a flicker noise floor of 4×10^{-16} per cavity.

Many components of the ^{199}Hg experiment have been described previously [15,16], so we only highlight a few elements below. Atoms are confined in a vertically orientated optical lattice loaded from a single stage magneto-optical trap (MOT). Once trapped and with the MOT fields off, we apply a Rabi light pulse at the $^1S_0 \leftrightarrow {}^3P_0$ transition frequency. At present we rely solely on ground state detection. There are $(2-3) \times 10^3$ atoms trapped in the lattice, from which a spectral line with ~11 Hz FWHM can be generated [14].

The source for the cooling light is a thin-disk Yb:YAG laser that is wavelength tuned using a birefringent filter and a temperature controlled etalon to 1014.902 nm. This light is frequency quadrupled through two resonant nonlinear optical cavities, the first producing ~3.5 W of 507.4 nm light and the second ~70 mW of 253.7 nm UV light. A challenging aspect of the mercury clock experiment is to produce a sufficiently deep optical lattice trap. The lattice light generation begins with ~900 mW of Ti:sapphire laser light that is frequency doubled in a resonant doubling cavity to produce 160 mW of 362.570 nm light near the magic wavelength, λ_m. The value of λ_m has previously been determined to within 3 ppm [14]. Two spherical mirrors with a radius of curvature equal to 250 mm and a reflectivity of 99.5% at 360 nm form the lattice buildup cavity. Here we produce 6.5(±0.7) W of intracavity circulating power. The waist of the cavity with $w_0(e^{-2}) = 120\ \mu$m coincides with the MOT atom cloud (the atom cloud can be displaced to optimize overlap with the lattice light), and the e^{-2} radius of the MOT atom cloud is ~110 μm prior to trap loading. Here we produce a lattice depth of 22 times the associated recoil energy, E_R (or ~8 μK in depth).

The light for probing the clock transition at 265.6 nm commences with a cavity stabilized fiber laser at 1062.6 nm that is frequency quadrupled through two resonant frequency doubling stages. To provide a probe signal with sufficiently narrow linewidth and high stability, the fiber laser is locked to an ultrastable optical cavity using Pound–Drever–Hall locking. Details of the system are presented in [17]. In Fig. 1 we show the

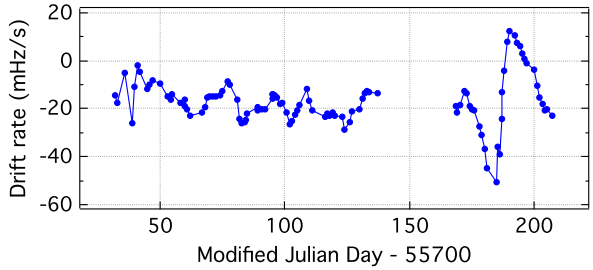

Fig. 1. (Color online) Frequency drift-rate record of a fiber laser at 1062.6 nm locked to an ultrastable cavity with a 10 cm length ULE spacer and fused-silica mirrors, recorded against the ^{199}Hg clock transition. The mean drift rate is -16.9 mHz s^{-1} (-6.0×10^{-17} s^{-1}).

frequency drift rate of the 1062.6 nm laser locked to the ultrastable cavity over a 6 month period (June 20 to December 12, 2011). The day-to-day drift rate is determined by comparisons with the ^{199}Hg clock transition. There are two characteristics of note. First, the absolute drift rate rarely rises above 30 mHz s^{-1}; the mean for the data in Fig. 1 is −16.9 mHz s^{-1}, or in fractional frequency terms -6.0×10^{-17} s^{-1}. The excursion seen at the end of the record is due to an abnormal temperature variation in the laboratory. Second, the drift rate is rarely positive, indicating that the cavity length is slowly lengthening over time, presumably due to creep in the optical cavity spacer [ultralow expansion glass (ULE)], which is orientated vertically.

To generate adequate power for the probe at 265.6 nm, about 400 μW of ultrastable laser (USL) light is used to injection lock a 250 mW distributed feedback semiconductor laser before carrying out the frequency quadrupling. Information regarding the frequency doubling resonant cavities is presented in [17]. Despite the very low drift rate exhibited by the USL, we find it accommodating to implement a drift cancellation scheme where a digital synthesizer is used to compensate the frequency drift of the probe light interacting with the atoms. The scheme is illustrated in Fig. 2. The frequency of the light reaching the atoms and that of the light received by a frequency comb experience the same fractional frequency drift cancellation (with a factor of 4 difference in absolute frequency). The 1062.6 nm laser light is delivered to the main Hg table and the frequency comb by way of polarization maintaining optical fiber, for which noise induced by the fiber is actively cancelled with an acousto-optic modulator (AOM). The frequency shift produced by the AOM 3 used in the noise suppression process also provides a means of sweeping the frequency of the probe light reaching the atoms with the aid of a computer to

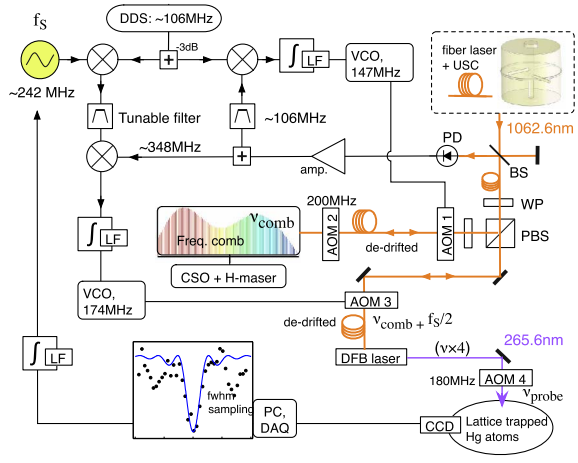

Fig. 2. (Color online) Scheme for locking to the ^{199}Hg clock line and measuring the line-center frequency. A data acquisition system is used to create a correction signal that is delivered to the $f_S\sim242$ MHz synthesizer, which controls the frequency of the probe light via AOM 3. AOM, acousto-optic modulator; CSO, cryogenic sapphire oscillator; DAQ, data acquisition and sequence control; DFB, distributed feedback diode laser; DDS, direct digital synthesizer; LF, loop filter; PBS, polarizing beam splitter; PD, photodiode; USC, ultrastable cavity; VCO, voltage controlled oscillator; WP, wave plate.

control a synthesizer (at $f_S\sim242$ MHz) in the control path of AOM 3. The computer records f_S, which is used to find the absolute frequency after incorporating the frequency comb measurements of the 1062.6 nm light and the offset from AOM 4, such that $\nu_{\rm probe}=4(\nu_{\rm comb}+f_S/2)-f_{\rm aom4}$ (refer to Fig. 2). The clock and cooling transitions are shown in the partial term diagram of Fig. 3(a). An example of the clock transition spectrum is seen in Fig. 3(b), obtained with a 50 ms duration square probe pulse and a cycle time $T_c=1.46$ s. The magnetic field strength $B\simeq0$ μT. The trace was averaged over $N=4$ scans. The Rabi angle for the line fit is 1.3π rad. From this data, we can estimate the cycle-to-cycle noise in the measurement of the transition probability to be $\sigma_{\delta P}=0.1$, which is $\sqrt{N}=2$ times larger than is apparent in Fig. 3(b) due to the averaging. Using the relationship

$$\sigma_y(\tau)=\frac{1}{\nu_{\rm Hg}}\frac{\sigma_{\delta P}}{dP/d\nu}\sqrt{\frac{T_c}{\tau}},\tag{1}$$

where $dP/d\nu$ is the maximum slope of the resonance, we can estimate the achievable fractional frequency stability, $\sigma_y(\tau)$, when locking to the ^{199}Hg line spectrum. With $dP/d\nu=0.02$ Hz^{-1}, we find $\sigma_y(\tau)\sim5.3\times10^{-15}/\sqrt{\tau}$.

By sampling the clock transition at the points of half-maxima (either side of center) we derive a correction signal that is delivered to AOM 3 (and AOM 1) of Fig. 2 via the synthesizer at f_S, so that the frequency of the probe light becomes locked to the ^{199}Hg clock transition. Our evaluation of the clock instability is essentially that of comparing the ^{199}Hg signal with the drift cancelled ultrastable laser. The frequency comb and microwave reference are only used to minimize the linear drift and can be excluded from the evaluation. The logged data of f_S is used for the stability measurements, converted to $\nu_{\rm probe}$ by using a mean value of $\nu_{\rm comb}$. This provides us with the inherent capability of the ^{199}Hg clock. An example of $\nu_{\rm probe}$ versus time is shown in Fig. 4(a), where the frequency is offset by that reported in [14]. The cycle time is 1.46 s, of which the MOT loading time is 1.32 s. The fractional frequency instability for this data [Fig. 4(b), filled circles] exhibits $\sigma_y(\tau)=5.4\times10^{-15}/\sqrt{\tau}$ out to 400 s, in good agreement with the instability predicted above.

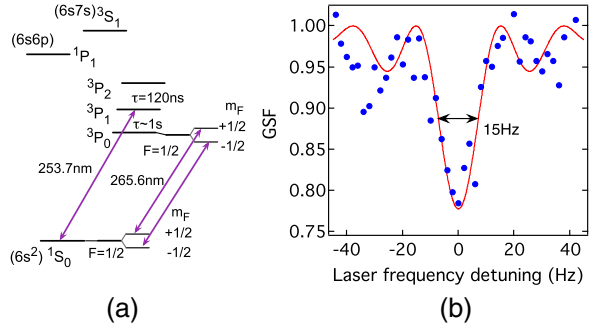

Fig. 3. (Color online) (a) Partial term diagram for ^{199}Hg showing the cooling (253.7 nm) and clock (265.6 nm) transitions, (b) ground state fraction versus probe laser detuning frequency for a 50 ms square probe pulse; (solid curve) curve fit with $\Omega\cdot T=1.3\pi$ rad.

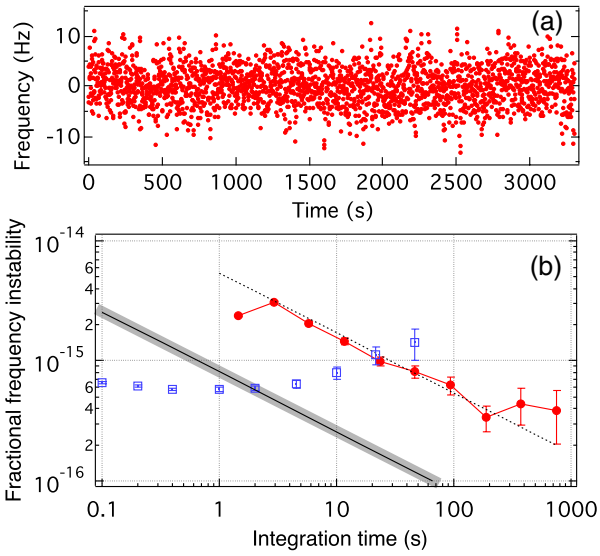

Fig. 4. (Color online) (a) ^{199}Hg frequency (offset by $\nu_{\mathrm{Hg}} = 1128575290808162.0$ Hz) versus time, (b) fractional frequency instability plot: ultrastable laser locked to the ^{199}Hg clock transition derived from f_S (filled circles), comparison between two ultrastable optical cavities (open squares), and Dick effect limited instability (solid line).

For comparison, an assessment of $\sigma_y(\tau)$ between two USL cavities is shown by the hollow squares of Fig. 4(b). One USL is that described above with $\lambda = 1062.6$ nm, while the other is a similar design, but has the ULE spacer orientated horizontally [18]. A separate Yb:fiber laser is locked to each cavity, having a frequency difference of ~1 GHz (the USLs are in separate laboratories). The minimum fractional instability obtained is 5.7×10^{-16}. Assuming equal contributions from the cavities, each exhibits a $\sigma_y(\tau) = 4.0 \times 10^{-16}$ flicker floor. We also show the limitation to $\sigma_y(\tau)$ set by the Dick effect for our present probe sequence. The calculation uses an estimation of the USL noise based on the measurement of Fig. 4(b) (hollow squares) along with earlier recorded USL versus H-maser data [17]. The limiting stability is $8.1 \times 10^{-16}/\sqrt{\tau}$, lying well below that shown for the ^{199}Hg resonance lock. These results show that further gains in the ^{199}Hg-locked laser frequency stability can be made by improving the signal-to-noise ratio (S/N) of the clock transition. At present the contrast of the clock resonance is ~20%. With a deeper lattice trap (e.g., with a reduced beam waist) and the use of atom number normalization methods, we expect to increase the contrast and S/N such that the very low Dick effect instability limitation is reached.

To conclude, we have demonstrated a fractional frequency instability of $5.4 \times 10^{-15}/\sqrt{\tau}$ for a 265.6 nm laser light locked to the clock transition of ^{199}Hg, and a short term instability of 5.7×10^{-16} between two lasers locked to separate 10 cm long cavities. One optical cavity exhibited a mean drift rate of -6.0×10^{-17} s^{-1} over a six month period, one of the lowest reported for optical cavities at room temperature [19]. We also show the first laser locking to a spectral line of ultracold neutral atoms in thedeep ultraviolet domain, to our knowledge. Based on 1 day's averaging, the fractional frequency uncertainties of various systematic shifts for the ^{199}Hg clock should reach into 10^{-17} the range.

The authors thank the Systèmes de Référence Temps-Espace technical support, in particular M. Lours and F. Cornu. This work is partly funded by IFRAF and CNES.

References

1. A. Ludlow, T. Zelevinsky, G. Campbell, S. Blatt, M. Boyd, M. de Miranda, M. Martin, L. Thomsen, S. Foreman, J. Ye, H. Fortier, E. Stalnaker, S. Diddams, Y. Le Coq, Z. Barber, N. Poli, H. Lemke, K. Beck, and C. Oates, Science **319**, 1805 (2008).
2. T. Rosenband, D. Hume, P. Schmidt, C. Chou, A. Brusch, L. Lorini, W. Oskay, R. Drullinger, T. Fortier, J. Stalnaker, S. Diddams, W. Swann, N. Newbury, W. Itano, D. Wineland, and J. Bergquist, Science **319**, 1808 (2008).
3. N. D. Lemke, A. D. Ludlow, Z. W. Barber, T. M. Fortier, S. A. Diddams, Y. Jiang, S. R. Jefferts, T. P. Heavner, T. E. Parker, and C. W. Oates, Phys. Rev. Lett. **103**, 063001 (2009).
4. C. W. Chou, D. B. Hume, J. C. J. Koelemeij, D. J. Wineland, and T. Rosenband, Phys. Rev. Lett. **104**, 070802 (2010).
5. N. Huntemann, M. Okhapkin, B. Lipphardt, S. Weyers, C. Tamm, and E. Peik, Phys. Rev. Lett. **108**, 090801 (2012).
6. C. W. Oates, E. A. Curtis, and L. Hollberg, Opt. Lett. **25**, 1603 (2000).
7. M. Takamoto, T. Takano, and H. Katori, Nat. Photon. **5**, 288 (2011).
8. Y. Jiang, A. Ludlow, N. Lemke, R. Fox, J. Sherman, L.-S. Ma, and C. Oates, Nat. Photon. **5**, 158 (2011).
9. S. G. Karshenboim and E. Peik, Eur. Phys. J. Spec. Topics **163**, 1 (2008).
10. O. Lopez, A. Haboucha, F. Kefelian, H. Jiang, B. Chanteau, V. Roncin, C. Chardonnet, A. Amy-Klein, and G. Santarelli, Opt. Express **18**, 16849 (2010).
11. K. Predehl, G. Grosche, S. M. F. Raupach, S. Droste, O. Terra, J. Alnis, T. Legero, T. W. Hänsch, T. Udem, R. Holzwarth, and H. Schnatz, Science **336**, 441 (2012).
12. D. Piester, A. Bauch, L. Breakiron, D. Matsakis, B. Blanzano, and O. Koudelka, Metrologia **45**, 185 (2008).
13. L. Cacciapuoti and C. Salomon, Eur. Phys. J. Spec. Topics **172**, 57 (2009).
14. J. J. McFerran, L. Yi, S. Mejri, S. Di Manno, W. Zhang, J. Guéna, Y. Le Coq, and S. Bize, Phys. Rev. Lett. **108**, 183004 (2012).
15. L. Yi, S. Mejri, J. J. McFerran, Y. Le Coq, and S. Bize, Phys. Rev. Lett. **106**, 073005 (2011).
16. S. Mejri, J. J. McFerran, L. Yi, Y. Le Coq, and S. Bize, Phys. Rev. A **84**, 032507 (2011).
17. S. T. Dawkins, R. Chicireanu, M. Petersen, J. Millo, D. V. Magalhaes, C. Mandache, Y. Le Coq, and S. Bize, Appl. Phys. B **99**, 41 (2010).
18. J. Millo, D. V. Magalhães, C. Mandache, Y. Le Coq, E. M. L. English, P. G. Westergaard, J. Lodewyck, S. Bize, P. Lemonde, and G. Santarelli, Phys. Rev. A **79**, 053829 (2009).
19. P. Dube, A. Madej, J. Bernard, L. Marmet, and A. Shiner, Appl. Phys. B: Lasers Opt. **95**, 43 (2009).